PHYSICAL REVIEW C VOLUME 14, NUMBER 2 AUGUST 1976

Neutron states in ^{195}Pt populated by the (d, p) and (d, t) reactions*

Y. Yamazaki and R. K. Sheline
Physics Department, Florida State University, Tallahassee, Florida 32306
(Received 26 January 1976)

The neutron states in ^{195}Pt have been studied using the ^{194}Pt$(d, p)^{195}$Pt and ^{196}Pt$(d, t)^{195}$Pt reactions and 12 and 13.5 MeV deuterons. Transfer l values have been determined from angular distributions, and spectroscopic factors obtained by comparison with distorted wave Born approximation calculations. Many lower energy states are well explained by the Nilsson model assuming an oblate nuclear shape. These include the $1/2^-[530]$, $3/2^-[532]$, $5/2^-[532]$, and decoupled $1/2^+[600]$ bands, and more tentatively the $3/2^-[541]$ and $9/2^+[615]$ bands. Other low-lying states are well described by the Faessler-Greiner model using parameters consistent with the ^{194}Pt data. The Coriolis force is important in reproducing the large spectroscopic factors experimentally observed. The success of the Faessler-Greiner and Davydov models in explaining the experimental ^{195}Pt spectra is also compared.

[NUCLEAR REACTIONS, NUCLEAR STRUCTURE ^{194}Pt(d,p), $E_d=12$ MeV. ^{196}Pt(d,t), $E_d=13.5$ MeV. Measured $\sigma(E_p, \theta)$, $\sigma(E_t, \theta)$, ^{195}Pt levels; deduced l, S; calculated J, π, S, rotation-vibration model. DWBA analysis, enriched targets.]

I. INTRODUCTION

The platinum isotopes are situated in a transition region between well-deformed and spherical nuclei. Studies of reorientation effects in Coulomb excitations suggest that nuclei change shape from prolate to oblate spheroids in the transition from the stable osmium to the stable platinum isotopes.[1-3] Since rotational bands built on high-spin unique-parity states in odd nuclei have been found to give detailed information on nuclear shapes and their changes,[4] these bands have been well studied experimentally in Ir, Pt, and Hg isotopes.[5-7] The observed spectra supported the results of the reorientation effects.

The first theoretical approach to states in ^{195}Pt was made by Hecht and Satchler[8] who extended the Davydov model[9] to odd nuclei. Experimentally, the states of ^{195}Pt have been fairly well studied from radioactive decay processes[10] and Coulomb excitations.[11] However, the single-nucleon transfer reactions to the platinum isotopes have only been investigated using targets with poor enrichment.[12-13] In the highly deformed region, single-nucleon transfer reactions have been one of the most powerful tools in identifying band members.[14] Although some additional complexity could be expected, this method should also prove powerful in this transition region. A lack of detailed data of this type seems to have discouraged additional attempts to describe the low-lying odd-parity states in terms of models since the work by Hecht and Satchler.[8]

The present investigation, then, was carried out in order to determine spectroscopic factors for the states in ^{195}Pt and to study whether it is possible to describe the states of the transitional nucleus in terms of any available models.

II. EXPERIMENTAL PROCEDURES

Targets of thickness $\simeq 50\,\mu g/cm^2$ were prepared by the vacuum evaporation of platinum metal, isotopically enriched to 97.4% in ^{194}Pt and 97.5% in ^{196}Pt onto $\simeq 50$-$\mu g/cm^2$ carbon foils. They were bombarded by 12- and 13.5-MeV deuteron beams from Florida State University (FSU) tandem Van de Graaff accelerator for the (d, p) and (d, t) reactions, respectively. Beam currents were typically about 1 μA on a target spot *0.3×3.0 mm² square*, and exposure times were 3 to 5 h for each angle. Scattered protons and tritons were detected photographically in 50-μm nuclear emulsions spring fitted on the focal surface of the FSU Browne-Buechner type spectrograph.[15] The proton spectra were recorded with aluminum absorbing foils placed in front of the emulsions to stop scattered deuterons.

The proton and triton tracks were counted in $\frac{1}{2}$-mm strips of the plates, and a least-squares fitting of the data was used, assuming the peak shape to be skewed Gaussian, in order to calculate both peak positions and areas. An energy scale was defined by assigning ground state peaks and carbon reference peaks in the (d, p) data and the ground state peaks and elastic reference peaks in the (d, t) data, respectively, using the Q values of the ^{194}Pt$(d, p)^{195}$Pt and ^{196}Pt$(d, t)^{195}$Pt reactions.[16] The peaks had a resolution of about 13 to 17 keV [full width at half maximum (FWHM)]. Since the exposure at each angle was accompanied by an

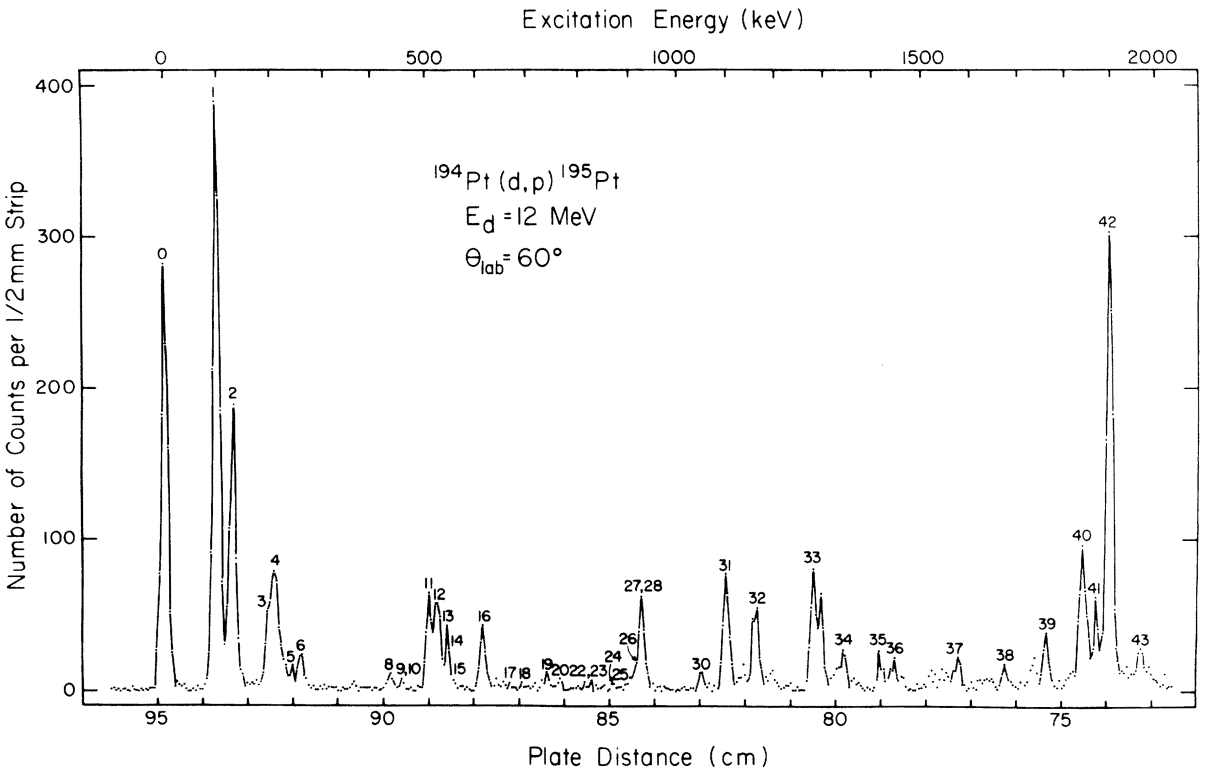

FIG. 1. Proton spectrum for the (d,p) reaction on ^{194}Pt at 60°.

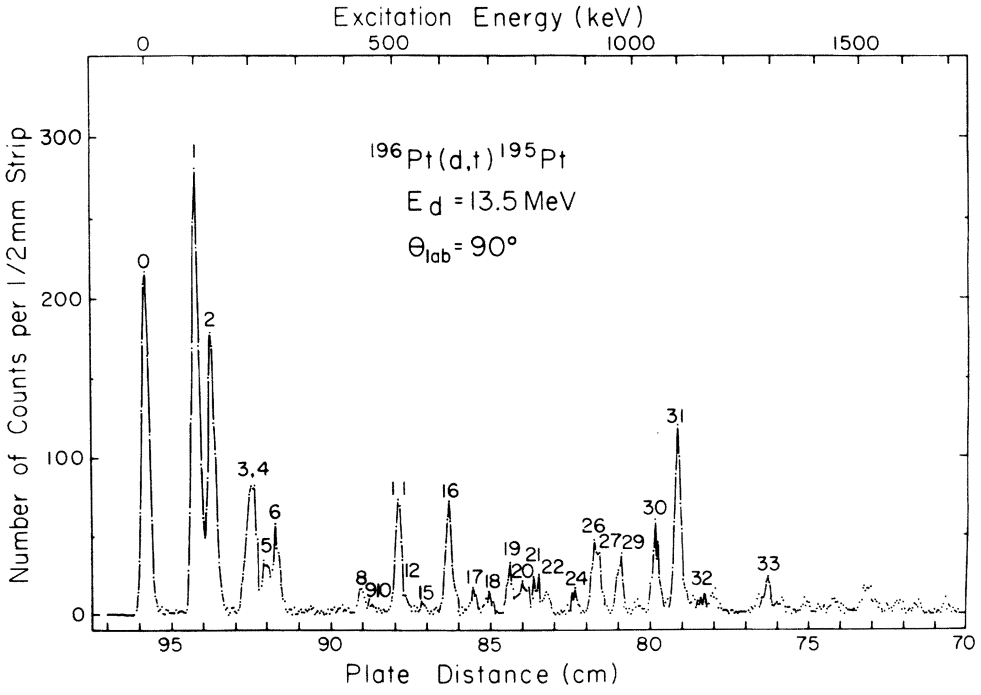

FIG. 2. Triton spectrum for the (d,t) reaction on ^{196}Pt at 90°.

elastic scattering measurement, the cross section of each peak observed was obtained as a relative value to an elastic scattering cross section at that angle. In a different run, an elastic scattering measurement was performed for seven different angles. Assuming that the elastic scattering at 25° is the same as the distorted wave Born approximation (DWBA) calculations (see Sec. III), which is 0.66% smaller than the Rutherford scattering at 12 MeV and 2.0% larger at 13.5 MeV, we determined the absolute cross sections of the (d,p) and (d,t) reactions.

III. EXPERIMENTAL RESULTS AND DWBA ANALYSIS

The states of ^{195}Pt were observed using the reaction ^{194}Pt$(d,p)^{195}$Pt at angles 35°, 50°, 60°, 80°, 100°, and 120° with an incident deuteron energy of 12 MeV, and using the reaction ^{196}Pt$(d,t)^{195}$Pt at angles 40°, 55°, 60°, 70°, 80°, and 90° with a deuteron energy of 13.5 MeV. Typical spectra of the (d,p) and (d,t) reactions are shown in Fig. 1 and Fig. 2, respectively. Light impurities were eliminated by their kinematic shifts, and heavy impurities were considered unlikely because of the >97% enrichment of the targets.

A series of DWBA calculations was carried out using the computer code DWUCK[17] to determine transferred l values and spectroscopic factors. For weakly excited states, the multistep processes were found to be important in some cases,[18] showing large deviations for angular distributions from those predicted by DWBA analyses. For strongly excited states, direct processes are dominant. If we use deuteron optical parameters which take into account inelastic absorption, DWBA analyses give results similar to those predicted by coupled channel analyses for strongly excited states fed by direct processes. In order to carry out the coupled channel analysis, it is necessary to assume a model for the nuclear structure which is unfortunately unknown at present. Therefore, rather simple DWBA analysis of the reaction data has been employed. It is suitable for the present purpose, if we keep in mind the possible ambiguities in the analysis and the discussion caused by multistep processes.

The optical model parameters used for the present DWBA calculations are listed in Table I. For the proton we used the optical model parameters derived from elastic scattering data of 13.76-MeV polarized protons on a ^{197}Au target.[19] For the deuterons we compared the results of two different sets of parameters derived from data of 12-MeV deuterons on ^{186}W and ^{208}Pb targets[19] with the observed angular distributions of the (d,p) reactions to the ground state, the 99-keV state, and the 130-keV state. The set of parameters used for ^{186}W listed in Table I yielded the better agreement. For the triton a comparison was made among several sets of parameters derived from 20-MeV triton elastic scatterings from ^{182}W, ^{207}Pb, and ^{208}Pb targets.[19] The set of triton parameters listed in Table I gave the best agreement with the present data. These exercises in choices of parameters may have been somewhat academic since there was at most only a 10% difference in the spectroscopic factors calculated with different parameter sets.

States of ^{195}Pt populated via the ^{194}Pt$(d,p)^{195}$Pt and the ^{196}Pt$(d,t)^{195}$Pt reactions are summarized in Table II together with the l-transfer values assigned by fitting the DWBA predictions to the experimental angular distributions. Comparison is also made between the present results and the previous radioactive decay results.[10] The angular distributions in which l-transfer values were fairly conclusively determined are shown in Fig. 3 for the stripping reaction and in Fig. 4 for the pickup reaction. Several angular distributions are shown in these two figures for states whose l assignments are less certain, but which will be important in the theoretical discussions. In those cases where there was overlap between levels observed in this research and in the decay work[10] all of the l-transfer values determined with a reasonable degree of certainty were consistent with spin-parity assignments from the

TABLE I. Optical-model parameters used in DWBA calculations. We used the values 0.625 and 0.845 as finite range parameters for the (d,p) and (d,t) reactions, respectively.

	V_0 (MeV)	r_0 (fm)	a (fm)	W_0 (MeV)	W' (MeV)	r_0' (fm)	a' (fm)	V_{so} (MeV)	r_{so} (fm)	a_{so} (fm)	r_C (fm)	β [a]
d	−85.92	1.15	0.892		+83.84	1.258	0.756				1.25	0.54
p	−58.33	1.23	0.72		+61.52	1.30	0.44	+22.8	0.95	0.92	1.19	0.85
t	−183.1	1.16	0.76	−21.6	0.0	1.332	0.994				1.25	0.20
n	b	1.25	0.65					+25.0				

[a] Nonlocal range parameter.
[b] Adjusted to reproduce the separation energy.

TABLE II. States populated in ^{195}Pt.

No.	Excitation energy (keV) (d,p)	(d,t)	Decay [c]	Transferred l (d,p)	(d,t)	J^π Decay [c]	Spect. factor [a,b] (d,p)	(d,t)
0	0.0	0.0	0.0	1	1	$\frac{1}{2}^-$	0.27	0.30
1	99.1(0.4)	99.1(0.3)	98.9	1	1	$\frac{3}{2}^-$	0.34	0.36
2	129.7(0.5)	129.9(0.4)	129.7	3	3	$\frac{5}{2}^-$	0.76	0.78
3	199(1)	199.7(0.7)	199.6	1	1	$\frac{3}{2}^-$	0.02	0.06
4	213(2)	212.2(0.6)	211.3		1	$\frac{3}{2}^-$	0.09	0.10
5	241(4)	238(1)	239.3		3	$\frac{5}{2}^-$	0.04	0.15
6	260(1)	259.4(0.7)	259.2	(6)	6	$\frac{13}{2}^+$	0.85	1.58
7	Not seen	Not seen	389.2			$(\frac{5}{2})^-$		
8	433(3)	431(1)	432.0		(4)	$(\frac{9}{2}, \frac{11}{2}, \frac{13}{2})^+$	0.04 [d]	0.08 [d]
9	Not seen	453(2) [e]	449.7		(3) [e]	$(\frac{5}{2}, \frac{7}{2})^-$		
10	Not seen		455.2			$(\frac{5}{2})^-$		0.02 [e]
11	507(1)	508.1(0.5)	507.9	3	3	$(\frac{5}{2}, \frac{7}{2})^-$	0.16 [f]	0.29 [f]
12	524(1)	Weak		1			0.04	
13	539(3)	Not seen						
14	548(3)	Not seen	547.0			$(\frac{11}{2})^+$		
15	Weak	Weak	562.6			$\frac{9}{2}^-$		
16	614(1)	612.6(0.5)	612.7	3	3	$(\frac{5}{2}, \frac{7}{2})^-$	0.10 [g]	0.22 [g]
17	Weak	663(2)						
18	Weak	694(1)	695.2		(3)	$(\frac{5}{2}, \frac{7}{2})^-$		0.05 [g]
19	Weak	738.9(0.6)			1			0.05
20	Weak	765.8(0.9)			3			0.07
21	Not seen	793(2)						
22	Weak	816(1)	814.6		(5)	$(\frac{9}{2})^-$		
23	Weak	Not seen	821.9					
24	Weak	875(1)						
25	Weak	Not seen	895.4					
26	Weak	915(1)						
27	930(1)	927.7(0.8)		1	(1–3)		0.03	0.04
28			930.7					
29	Not seen	971.3(0.8)			3			0.13
30	Weak	1049.3(0.7)						
31	1100(1)	1098(1)		1	(1)		0.04	0.13
32	1159(1)	1156(2)		(3, 4)	(3, 4)			
33	1294(1)			1			0.03	
34	1337(2)							
35	1420(2)			(1)				
36	1445(3)							
37	1577(2)			1			0.01	
38	1681(3)							

TABLE II. *(Continued)*

No.	Excitation energy (keV) (d,p)	(d,t)	Decay [c]	Transferred l (d,p)	(d,t)	J^π Decay [c]	Spect. factor [a,b] (d,p)	(d,t)
39	1766(2)			(1)				
40	1840(2)			1			0.04	
41	1872(2)			(3)				
42	1899(1)			(3, 4)			0.85 [d]	
43	1972(3)			1			0.02	

[a] Listed only for the states whose l assignments were considered to be definite.
[b] Extracted from Eq. (1).
[c] Reference 10.
[d] Calculated assuming the spin-parity to be $\frac{9}{2}^+$.
[e] Unresolved peak.
[f] Calculated assuming the spin-parity to be $\frac{5}{2}^-$.
[g] Calculated assuming the spin-parity to be $\frac{7}{2}^-$.

decay work.[10]

The spectroscopic factor S is given by

$$\frac{d\sigma}{d\Omega} = 2NS\sigma^{l}_{\mathrm{DW}}(\theta), \qquad (1)$$

where N is a normalization factor and $\sigma^{l}_{\mathrm{DW}}(\theta)$ is obtained from the DWBA calculations. The spectroscopic factors obtained using this equation are listed in Table II. For the normalization factor N for the (d,p) and (d,t) reactions, the usual values $N=1.53$ and $N=3.33$ were used, respectively.

IV. DISCUSSIONS OF THE RESULTS

In the highly deformed region, the empirical spectroscopic factors, extracted using Eq. (1), are usually in approximate agreement with the values given by the Nilsson model, particularly for strongly excited states. However, this agreement cannot be expected *a priori*. As a matter

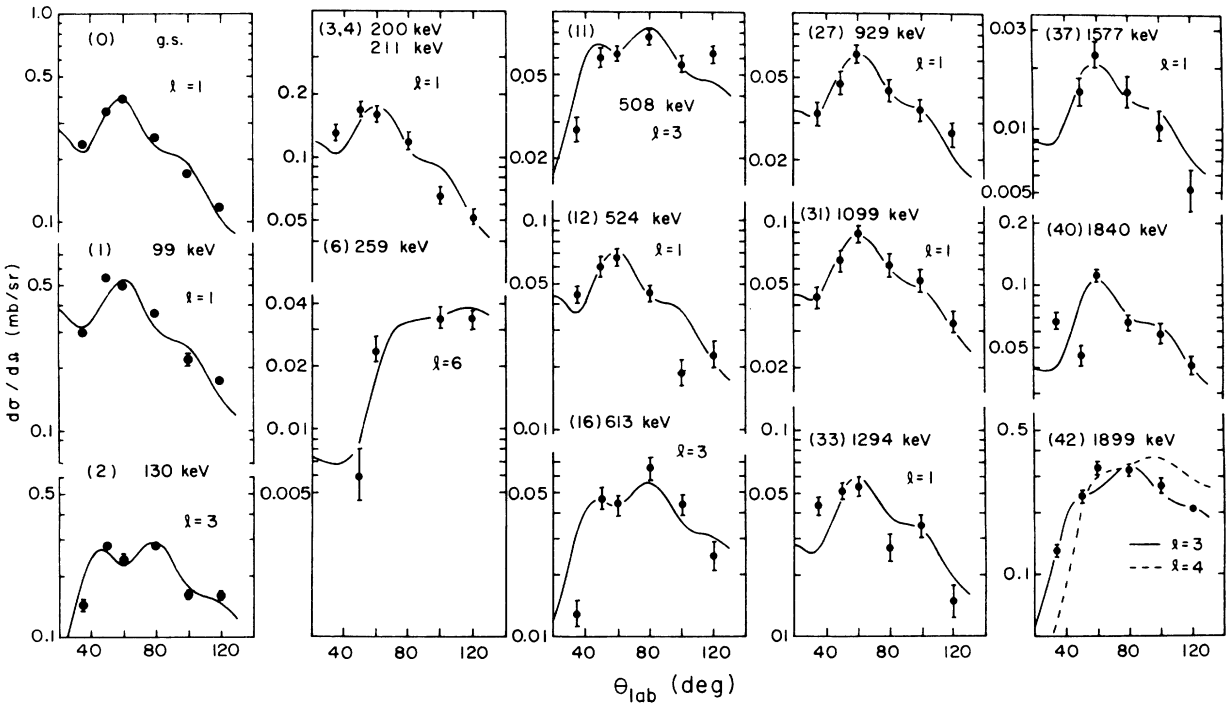

FIG. 3. Angular distributions for transitions in the ^{194}Pt$(d,p)^{195}$Pt reaction at 12.0 MeV. The curves are the result of the DWBA calculations.

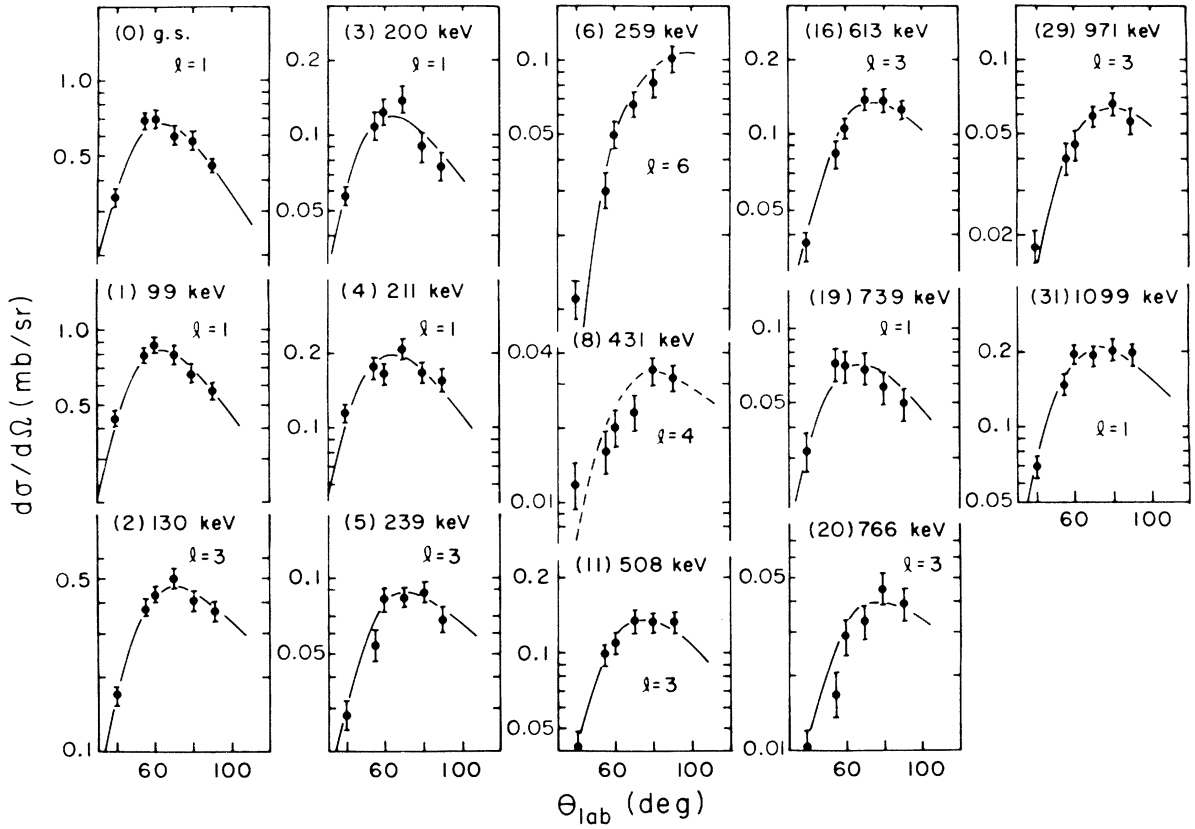

FIG. 4. Angular distributions for transitions in the ^{196}Pt$(d,t)^{195}$Pt reaction at 13.5 MeV. The curves are the result of the DWBA calculations.

of fact, the extracted spectroscopic factors occasionally deviate from theory by a large factor for weakly excited states. This fact has been explained as an effect of the multistep process mentioned in the previous section.[18] Therefore in our calculations we tried to reproduce only the relatively reliable spectroscopic factors for the strongly excited states, in addition to the excitation energies, with available models.

A. Interpretation of the present experimental results in terms of the Nilsson (Ref. 20) and the Faessler-Greiner models (Refs. 21 and 22)

Studies of reorientation effects in Coulomb excitation indicate that the heavier even platinum isotopes have oblate shapes.[1-3] In addition, decoupled bands built on the $i_{13/2}$ hole orbital have been found in the lighter platinum isotopes.[6] It is well known that rotational bands of high-spin unique-parity hole states become decoupled bands only in oblate nuclei in this region of the nuclear Periodic Table.[4] Therefore, ^{195}Pt is expected to be oblate.

One of the most characteristic features of the present experimental data is that the lowest $\frac{1}{2}^-$, $\frac{3}{2}^-$, and $\frac{5}{2}^-$ states are strongly populated; they have 57%, 35%, and 51% of the full single-particle strengths, respectively. As shown in Fig. 5 assuming negative β, there are three Nilsson orbitals $\frac{1}{2}^-[530]$, $\frac{3}{2}^-[532]$, and $\frac{5}{2}^-[532]$ near the Fermi surface with the appropriate spin-parity. In each case, the $p_{1/2}$, $p_{3/2}$, and $f_{5/2}$ components of those orbitals are predicted to be quite large. This suggests that the lowest three states are bandheads built on these three orbitals.

The sum of the spectroscopic factors for the (d,p) and (d,t) reactions is larger than unity for the 130- and 259-keV states. This fact indicates that the Coriolis force will play an important role in the interpretation of the present experimental results. The Coriolis calculation including the five odd-parity and five even-parity Nilsson orbitals near the Fermi surface has been carried out with the moment of inertia parameter derived from the excitation energy of the first 2^+ state in ^{194}Pt. The strength of the pairing interaction[23,24] was determined in such a way that it yields the gap parameter necessary to reproduce the odd-even mass difference. An attenuation factor of 0.7 was used for the Coriolis force. In order to reproduce the bandhead energies we have

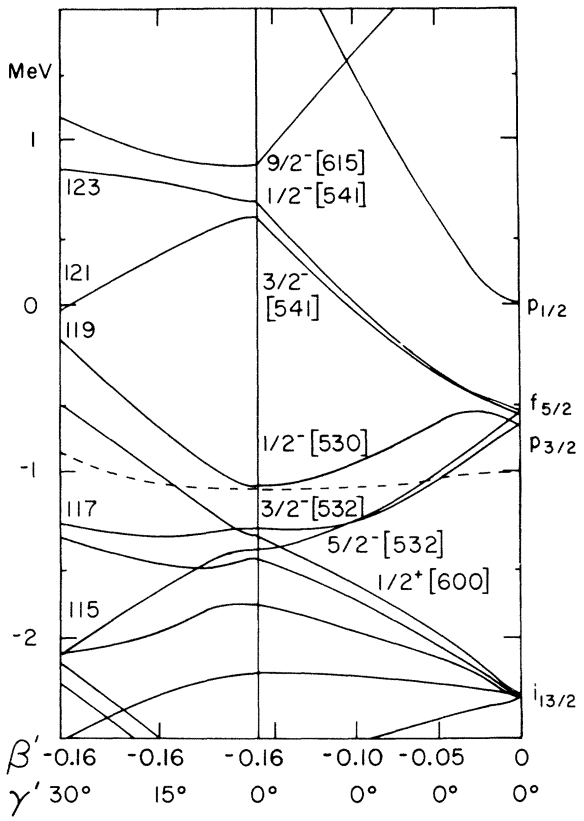

FIG. 5. Single-particle states for odd-neutron nuclei in the transition region. Since this diagram is for an oblate nucleus, $\beta' = -\beta$, $\gamma' = 60° - \gamma$, if we use the usual notation for the β and γ planes. In the calculation, we used the following single-particle energies at the spherical limit: $\epsilon(p_{1/2}) = 0.0$, $\epsilon(p_{3/2}) = -0.732$, $\epsilon(f_{5/2}) = -0.654$, $\epsilon(f_{7/2}) = -3.251$, $\epsilon(h_{9/2}) = -3.584$, $\epsilon(g_{9/2}) = +2.706$, and $\epsilon(i_{13/2}) = -2.367$ (MeV).

also modified slightly the single-particle energies of the spherical limit. In this way we obtained fairly good agreement with the experiment for both of the bandhead energies and the spectroscopic factors as shown in Table III.

However, there were three difficulties in using the Nilsson model to explain the experimental results. First, we had to use a deformation parameter $\beta = -0.13$ rather than $\beta = -0.16$ derived from the $B(E2)$ value of the 2^+ to 0^+ transition in ^{194}Pt. Second, the predicted energies of the $\frac{7}{2}^-$ and $\frac{9}{2}^-$ states were much higher than the observed excitation energies. Third, the presence of many states between 500 and 1000 keV could not be explained.

In the even isotopes of Os, Pt, and Hg, an extremely low-lying second 2^+ state has been observed systematically. In addition, the high-spin states of the ground band are appreciably depressed compared with the prediction of the symmetric rotator model. These facts suggest an additional model possibility—an extremely soft γ-fluctuating nucleus approaching γ instability. Results of calculations of potential energy surfaces show only shallow minima in the β and γ plane in this transition region.[25] Taking into account the effects of β and γ vibrations, Faessler and Greiner were able to explain both the low-lying spectra and the transition probabilities in the even-even nuclei of this region.[21,22] In order to resolve the three difficulties in using the Nilsson model, we have carried out a calculation using the Faessler-Greiner model.

The present calculation took into account the Coriolis, rotation-vibration and particle-vibration couplings, including the five odd-parity Nilsson orbitals and the seven even-parity orbitals near the Fermi surface. Effects of the higher excitations such as two phonon γ vibrations and β vibrations were neglected. The result is compared with the experiment in Fig. 6 and in Table III. The vibrational energy E_γ and moment of inertia were chosen so as to reproduce the energies of the first and second excited 2^+ states in ^{194}Pt, while the deformation parameter β was derived from the measured $B(E2)$ value for the ^{194}Pt 2_1^+ to 0^+ ground state transition. The same values as the Nilsson model calculation were used for the pairing interaction, the single-particle energies of the spherical limit, and the attenuation factor of the Coriolis force.

It was found necessary to reduce the quasiparticle energy of $\frac{3}{2}^-[541]$ by 500 keV, and to increase those of the even-parity states originating from the $i_{13/2}$ state. Because of these difficulties the assignment of $\frac{3}{2}^-[541]$ is considered to be tentative. On the other hand, the elevation of the even-parity decoupled band may be understood as a result of specific pairing interactions involving this high-spin state, which may energetically prefer a pair in the $i_{13/2}$ orbital rather than the lower-spin orbitals. A similar situation is well known for the $\frac{11}{2}^-$ proton state in the well-deformed region.[14,26]

The parameters determined from the ^{194}Pt data suggest that the ^{194}Pt core is extremely soft with a large zero-point vibration amplitude $\langle \gamma^2 \rangle^{1/2} \simeq 30°$. Since the band concept is not valid for large band mixtures, the Nilsson assignments shown in the Fig. 6 and the Table III should be considered as asymptotic quantum numbers in the symmetrical limit. For instance, the main components of the states higher than 600 keV have fractional parentages less than 50%. Although these states are obviously very complex, they are presented for convenience in Fig. 6 as the bands whose component is the largest.

In spite of this softness, the nature of the states

TABLE III. Band assignment and spectroscopic factors for states in ^{195}Pt.

Band	Energy (keV)	Assigned l	Assigned J^π	Spectroscopic factors (d,p) Exp.	(d,p) Predicted a	(d,p) Predicted b	(d,t) Exp.	(d,t) Predicted a	(d,t) Predicted b
$\frac{1}{2}^-[530]$	0	1	$\frac{1}{2}^-$	0.27	0.28	0.30	0.30	0.25	0.27
	211	1	$\frac{3}{2}^-$	0.09	0.08	0.10	0.10	0.01	0.03
	239	3	$\frac{5}{2}^-$	0.04	0.21	0.11	0.15	0.03	0.02
	695	3	$(\frac{7}{2})^-$	Weak	0.02	0.02	0.05	c	···
	815	(5)	$(\frac{9}{2})^-$	Weak	0.02	0.01	Weak	···	···
$\frac{3}{2}^-[532]$	99	1	$\frac{3}{2}^-$	0.34	0.42	0.36	0.36	0.42	0.52
	389		$(\frac{5}{2})^-$	···	0.03	···	···	0.04	···
	613	3	$(\frac{7}{2})^-$	0.10	0.16	0.13	0.22	0.12	0.14
	931		$(\frac{9}{2})^-$	Weak	0.03	···	Weak	0.04	···
$\frac{5}{2}^-[532]$	130	3	$\frac{5}{2}^-$	0.76	0.73	0.57	0.78	0.75	0.75
	450	(3)	$(\frac{7}{2})^-$	Weak	0.01	···	0.02	0.01	···
	563		$\frac{9}{2}^-$	Weak	0.10	0.22	···	0.07	0.21
$\frac{3}{2}^-[541]$ [d]	200	1	$\frac{3}{2}^-$	0.02	···	0.01	0.06	0.03	···
	508	3	$(\frac{5}{2})^-$	0.16	0.17	0.71	0.29	0.02	0.01
	766	3	$(\frac{7}{2})^-$	Weak	0.03	···	0.07	0.02	···
$\frac{1}{2}^+[600]$ [e]	259	6	$\frac{13}{2}^+$	0.85	0.35	0.70	1.58	3.06	3.27
	433	(4)	$(\frac{9}{2})^+$	0.04	0.02	0.03	0.08	0.11	0.11
$\frac{9}{2}^+[615]$	1899	(4)	$(\frac{9}{2})^+$	0.85	0.92				

[a] Predicted by Faessler-Greiner model.
[b] Predicted by Nilsson model.
[c] Less than 0.01.
[d] Tentative assignment.
[e] Decoupled band.

lower than 600 keV can be understood in terms of the Nilsson model as well. In our picture of the Faessler-Greiner model, single particles feel the $Y_{2\pm2}$ force as a fluctuation in the equilibrium symmetric field, represented by small admixtures of $|K-\Omega| \geq 2$ for the lower excited states. The difference between the two models can be detected in the states higher than the vibrational excitations. With the Faessler-Greiner model, the natures of these states could be described well with the parameters consistent with the ^{194}Pt spectroscopic data.

Therefore, the states below 600 keV were assigned as members of the following Nilsson bands.

1. $\frac{1}{2}^-[530]$ band

Both the Nilsson and Faessler-Greiner model calculations predict that the ground state should be the bandhead of the $\frac{1}{2}^-[530]$ band with spectroscopic factors $S(d,p) \simeq 0.28$ and $S(d,t) \simeq 0.25$. The experimentally determined spin-parity and spectroscopic factors of the ground state are consistent with this prediction.

Candidates for a $\frac{5}{2}^-$ member of the ground state band are provided by the 130- and 239-keV states, both strongly connected with the ground state by $E2$ transitions. However, the 130-KeV state was populated in both the (d,p) and (d,t) reactions so strongly that it should be assigned as the $\frac{5}{2}^-[532]$ bandhead arising from the $f_{5/2}$ shell. Hence, the state at 239 keV is identified as the $\frac{5}{2}^-$ member of the $\frac{1}{2}^-[530]$ band. This assignment produces good agreement between the observed and predicted excitation energies (see Fig. 6).

The $\frac{5}{2}^-$ member decays to two $\frac{3}{2}^-$ states at 99 and 211 keV which can be candidates for a $\frac{3}{2}^-$ member of the $\frac{1}{2}^-[530]$ band. The former was populated

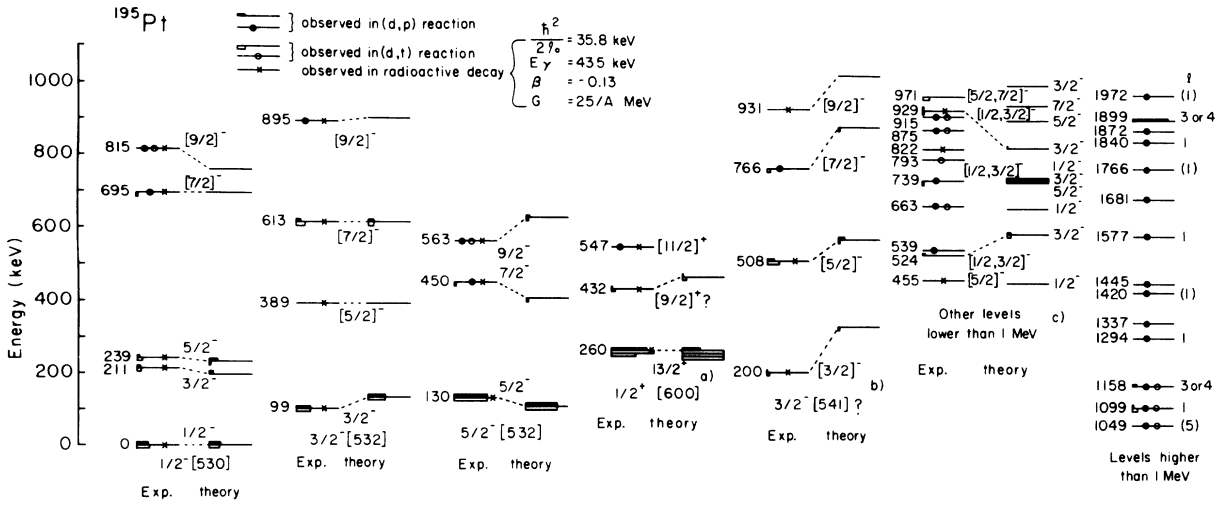

FIG. 6. Summary of the states of ^{195}Pt observed in the present work and radioactive decay studies. Comparison is made with a prediction by Faessler-Greiner rotation-vibration model. Spectroscopic factors of the (d,p) and (d,t) reactions are designated by lengths of dark heavy lines and open heavy lines, respectively, while lengths of thin lines correspond to unity. For states higher than 613 keV, the concept of bands is not valid, but the main components of the states are designated as band members.

strongly via the (d,p) and (d,t) reactions as predicted for the $\frac{3}{2}^-[532]$ bandhead. Therefore, the 211-keV state is assigned as a $\frac{3}{2}^-$ member of the $\frac{1}{2}^-[530]$ band.

Although both of the models reproduced the experimental energies of the $\frac{3}{2}^-$ and $\frac{5}{2}^-$ members of the ground state band with parameters consistent with the ^{194}Pt core spectrum (see Fig. 6), the predicted spectroscopic factors for these two states deviated from the measurement. The multistep process through the inelastic channel may be particularly important for the transitions to the $\frac{3}{2}^-$ and $\frac{5}{2}^-$ states, since the predicted spectroscopic factor suggests that the direct feeding of these states is not predominant.

2. $\frac{3}{2}^-[532]$ band

The $\frac{3}{2}^-$ bandhead was predicted at 133 keV with the Faessler-Greiner model, and experimentally observed at 99 keV. The extreme strength of population of this state via the (d,p) and (d,t) reactions is consistent with theory. The transition from the 389-keV $\frac{5}{2}^-$ state to the $\frac{3}{2}^-$ bandhead was the strongest among the $\frac{5}{2}^-$ states.[10] The predicted energy is consistent with the assignment of the 389-keV state as a $\frac{5}{2}^-$ member of this band.

3. $\frac{5}{2}^-[532]$ band

The predicted energy and extremely large spectroscopic factor are consistent with the assignment of 130 keV as the $\frac{5}{2}^-[532]$ bandhead. The sum of (d,p) and (d,t) spectroscopic factors larger than unity can be understood as a result of Coriolis coupling. The 450- and 563-keV states decayed strongly to 130-keV bandhead,[10] and were assigned as the $\frac{7}{2}^-$ and $\frac{9}{2}^-$ band members, respectively. These energies agree well with those calculated.

4. $\frac{3}{2}^-[541]$ band

The assignment of the 200-keV $\frac{3}{2}^-$ state and 508-keV state to the $\frac{3}{2}^-[541]$ band remains tentative, because we had to reduce the quasiparticle energy of this intrinsic state by approximately 500 keV. With this reduction, the theory can correctly predict the spectroscopic factors except for the $S(d,t)$ of the 508-keV state. However the energies cannot be reproduced because of the repulsion between this band and the $\frac{1}{2}^-[530]$ band.

5. $\frac{1}{2}^+[600]$ band

Among the even-parity states, the $\frac{13}{2}^+$ state was the lowest, and populated very strongly; $S(d,p) = 0.85$ and $S(d,t) = 1.58$. The larger (d,t) spectroscopic factor indicates that the state is a hole state, and the fact that $S(d,p) + S(d,t) = 2.43 > 1.0$ excludes the possibility that it is a normal bandhead. In oblate nuclei, rotational bands of high-spin unique-parity hole states are known to be decoupled. Coriolis coupling plays an important role in concentrating the strength of the single-particle transfer reaction in the bandhead.[4] Therefore, the present experimental result justifies the assignment of the $\frac{13}{2}^+$ state as the bandhead of the decoupled band in agreement with assignments in the lighter platinum isotopes.[6]

The spin-parity of the 433-keV state was pre-

viously assigned from the decay work as an $(\frac{11}{2}, \frac{13}{2})^+$ state.[10] However, the possibility of a $\frac{9}{2}^+$ assignment could not be completely rejected from decay work. Unfortunately, the angular distribution of the present work does not determine the l value of this state because of poor statistics (see Fig. 4). If we assume a $\frac{9}{2}^+$ asignment, the energy and spectroscopic factor can easily be understood by assigning it as a member of $\frac{1}{2}^+[600]$ decoupled band. The presence of an $(\frac{11}{2}, \frac{13}{2})^+$ state at so low an energy as previously assigned cannot be easily understood.

6. $\frac{9}{2}^+[615]$ band

At 1899 keV there is an extremely intense peak in the (d,p) spectrum whose l-transfer value was assigned to be $l=3$ or 4 (see Fig. 3). A possible candidate for this state is the bandhead of the $\frac{9}{2}^+$ [615] band, whose energy and spectroscopic factor agreed well with this prediction. The assumption of even-parity is necessary to understand such an intense peak at the high excitation energy, because the strength of the transfer reactions will be distributed among many states in the case of odd parity.

7. Other states

Between 613 and 930 keV there are three $\frac{7}{2}^-$ and three $\frac{9}{2}^-$ states. The Faessler-Greiner model predicts the energies of these states fairly well. Their wave functions are too complicated to be assigned as single band members. Experimentally, these states decay to many states which belong to different bands,[10] while their neutron transfer cross sections are small. Although the Nilsson model is capable of describing the properties of many of the low-lying states, it cannot reproduce these low energies for the $\frac{7}{2}^-$ and $\frac{9}{2}^-$ states. We have adopted the criterion that states are given band assignments consistent with the largest theoretical components in their wave functions, even though the absolute values of these components are small. The result of this kind of assignment is shown in Table III and Fig. 6.

In addition to these six states, many states with small cross sections are observed between 500 and 1000 keV as expected from the Faessler-Greiner model.

It should be noticed that assignments such as $\frac{1}{2}^-[530]\otimes 2^+$ are quite impossible because of strong rotation-vibration, particle-rotation, and particle-vibration couplings, although the softness of the nucleus did not have appreciable effects on states much lower than the vibration energy.

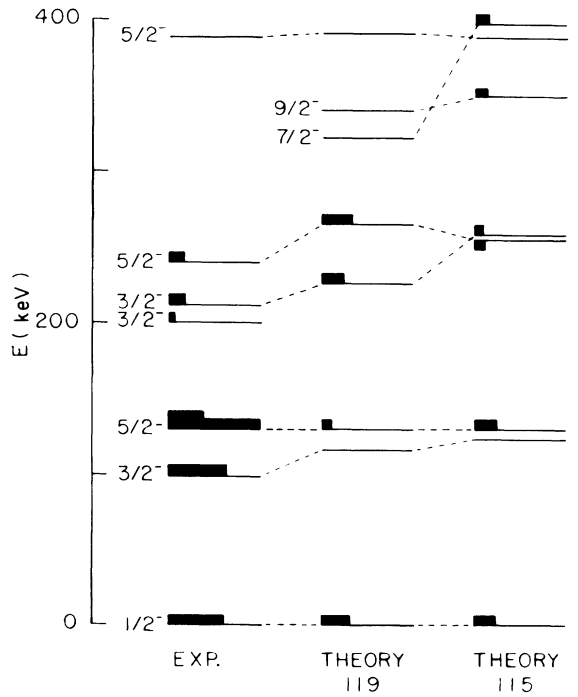

FIG. 7. Comparison of the experimental result with the prediction by the Davydov model at $\beta=0.16$ and $\gamma=30°$. The moment of inertia was chosen to fit the 130-keV state. For the label 115 and 119, see Fig. 5. The sum of spectroscopic factors for the (d,p) and (d,t) reactions are indicated by lengths of heavy lines, while lengths of thin lines correspond to unity.

B. Comparison with the Davydov model (Ref. 9)

The experimental data for even-even nuclei in this transitional region, suggesting the possibility of soft γ-fluctuating nuclei, have previously been reproduced by Davydov and Fillipov[9] assuming an asymmetric deformation. In addition, the rotational bands built on high-spin unique-parity states have recently been interpreted in terms of an asymmetric deformation.[27,28] In Fig. 5, intrinsic single-particle orbitals for odd-neutron nuclei are illustrated for the asymmetric field in addition to the Nilsson diagram. Applying the Davydov model[9] to the spectrum and the $B(E2)$ value of ^{194}Pt, the values of $\beta=0.16$ and $\gamma=30°$ were obtained. With these parameters, the energies of the low-lying spectrum in ^{195}Pt were reproduced with the asymmetric rotator model as shown in Fig. 7. Indeed, two different schemes (115 and 119 of Fig. 7) each involving different intrinsic states (115 and 119 of Fig. 5) can reproduce the energies. The moment of inertia parameter was chosen to fit the 130-keV state and mixing among the intrinsic particle orbitals was neglected (adiabatic strong coupling model). Therefore, this result is essentially the same as calculated by Hecht and Satchler.[8]

The strengths of the experimental neutron transfer reactions were then compared with the sums of the stripping and pickup spectroscopic factors of the asymmetric rotor model calculation. One of the most striking features of this comparison is that the lowest $\frac{3}{2}^-$ state, strongly excited in the experiment, is not expected to be strongly excited in either of the two rotational band interpretations. It has previously been pointed out[8] that this model cannot give the observed values of the $M1$ and $E2$ transition probabilities, assuming that all of the three states are members of a single rotational band. Consequently, the present experimental result implies that the low-lying $\frac{1}{2}^-$, $\frac{3}{2}^-$, and $\frac{5}{2}^-$ states each involve separate intrinsic excitations, if the Davydov model is applicable. Strong mixtures of the different intrinsic states are then expected, because the particle excitations are then lower than the rotational excitations.

The possibility that the Davydov model could describe the experimental results was therefore investigated assuming a mixture among five asymmetric rotational bands. Values of β, γ, and moment of inertia derived from the ^{194}Pt core were used. The pairing calculation has been performed for intrinsic orbitals in the asymmetric field of $\gamma = 30°$. The calculated result did not give a satisfactory fit to the large cross sections experimentally observed for the lowest three states. Unfortunately, the present analysis cannot reject the possibility of the Davydov model completely because of difficulties in the parameter search.

It should be noticed that the success of the Faessler-Greiner model in the present analysis is not inconsistent with the applicability of the Davydov model[27, 28] to approximately pure particle or hole unique-parity states. In these cases, the Davydov model is similar to the Faessler-Greiner model as can be understood from the formulation of Hamiltonians. As a matter of fact, it has been shown by Tanaka and Sheline[29] that the differences between the two models are not enough to clearly distinquish which model is more applicable. On the other hand, the two models can yield differences for orbitals near the Fermi surface because of the pairing interaction.

V. CONCLUSION

Analysis of the present experimental results indicates that the Faessler-Greiner model[21,22] is fairly successful in describing the nature of the states in the transitional nucleus ^{195}Pt with parameters consistent with the spectroscopic data from the ^{194}Pt core. Since the lowest $\frac{1}{2}^-$, $\frac{3}{2}^-$, $\frac{5}{2}^-$, and $\frac{13}{2}^+$ states have quite large spectroscopic factors, the Coriolis force is found to play an important role. The Faessler-Greiner model is based on an interpretation of the extremely low-lying second 2^+ state in the even-even core nuclei as arising from a γ fluctuation with large amplitude. The success of this model supports calculations of potential energy surfaces with no sharp minima in the β-γ plane.[25]

The results presented here also justify a limited validity of the Nilsson model for several states, in spite of fluctuating nuclear shapes. Thus, the identification of the $\frac{1}{2}^-[530]$, $\frac{3}{2}^-[532]$, $\frac{5}{2}^-[532]$, and decoupled $\frac{1}{2}^+[600]$ bands have been established, while the $\frac{3}{2}^-[541]$ and $\frac{9}{2}^+[615]$ bands are tentatively identified. The Faessler-Greiner model can also explain the observed energies of the $\frac{7}{2}^-$ and $\frac{9}{2}^-$ states whose complexity excludes their interpretation as band members, and also provides candidates for many observed states in the energy range less than 1 MeV which cannot be reproduced by the Nilsson model.

The present experimental result rejects an interpretation of the low-lying states as members of a single asymmetric rotational band as proposed by Hecht and Satchler.[8] The asymmetric rotor model, with mixtures of the different bands taken into account, did not give a satisfactory agreement between experiment and theory. However, it is difficult to reject the possibility of this model, since there are too many adjustable parameters in this case.

ACKNOWLEDGMENTS

We would like to thank Dr. Y. Tanaka for his advice and assistance in developing a computer code for the Davydov model and the Faessler-Greiner model and for his stimulating discussions about the interpretation of the experimental results. We are very grateful to Mr. B. Leonard for the target preparation and would like to acknowledge the assistance of Mr. R. Lasijo, Mr. R. Bagnell, Mr. C. Atwood, Mr. G. Green, and Mrs. M. Hoehn in helping to take the data. The careful work of Mrs. L. Wright and Miss R. Schedel in scanning the emulsion exposure is appreciated. Finally, we would like to thank Dr. K. Chapman, Mr. S. Trimble, and Mr. L. Rowton for the maintenance of the accelerator.

*Supported by ERDA contract (40-1)-2434 between the Florida State University and the U.S. Energy Research and Development Administration.

[1]J. E. Glenn, R. J. Pryor, and J. X. Saladin, Phys. Rev. 188, 1905 (1969).
[2]R. J. Pryor and J. X. Saladin, Phys. Rev. C 1, 1573 (1970).
[3]S. A. Lane and J. X. Saladin, Phys. Rev. C 6, 613 (1972).
[4]F. S. Stephens, R. M. Diamond, J. R. Leigh, T. Kammuri, and K. Nakai, Phys. Rev. Lett. 29, 438 (1972).
[5]S. Andre, J. Boutet, J. Jastrzebski, J. Lukasiak, J. Rivier, C. Sebille-Schuck, Z. Sujkowski, and J. Treherne, in *Proceedings of the International Conference on Nuclear Physics, Munich, Germany, 1973*, edited by J. de Boer and H. J. Mang (North-Holland, Amsterdam/American Elsevier, New York, 1973), p. 196.
[6]M. Piiparinen, J. C. Cunnane, P. J. Daly, C. L. Dors, F. M. Bernthal, and T. L. Khoo, Phys. Rev. Lett. 34, 1110 (1975).
[7]H. Beuscher, W. F. Davidson, R. M. Lieder, A. Neskakis, and C. Mayer-Boricke, Phys. Rev. Lett. 32, 843 (1974).
[8]K. T. Hecht and G. R. Satchler, Nucl. Phys. 32, 286 (1962).
[9]A. S. Davydov and G. F. Fillipov, Nucl. Phys. 8, 237 (1958).
[10]J. F. W. Jansen, A. Faas, and W. J. B. Winter, Z. Phys. 261, 95 (1973).
[11]R. Barloutaud, T. Grjebine, P. Lehmann, A. Leveque, J. Quidort, and G. M. Temmer, J. Phys. Radium 19, 570 (1958).
[12]P. Mukherjee, Nucl. Phys. 64, 65 (1965).
[13]M. J. Martin, Nucl. Data B8, 431 (1972).
[14]M. E. Bunker and C. W. Reich, Rev. Mod. Phys. 43, 348 (1971).
[15]C. P. Browne and W. W. Buechner, Rev. Sci. Instrum. 27, 899 (1956).
[16]N. B. Gove and A. H. Wapstra, Nucl. Data A11, 127 (1972).
[17]P. D. Kunz, computer program DWUCK, University of Colorado, 1967 (unpublished).
[18]R. J. Ascuitto, C. H. King, L. J. McVay, and B. Sorensen, Nucl. Phys. A226, 454 (1974).
[19]C. M. Perey and F. G. Perey, At. Data Nucl. Data Tables 13, 293 (1974).
[20]S. G. Nilsson, K. Dan. Vidensk. Selsk. Mat. Fys. Medd. 29, No. 16 (1955).
[21]A. Faessler and W. Greiner, Z. Phys. 168, 425 (1962); 170, 105 (1962); 177, 190 (1964).
[22]J. M. Eisenberg and W. Greiner, *Nuclear Theory* (North-Holland, Amsterdam, 1970), Vol. 1.
[23]S. T. Belyaev, K. Dan. Vidensk. Selsk. Mat. Fys. Medd. 31, No. 11 (1959).
[24]L. S. Kisslinger and R. A. Sorensen, K. Dan. Vidensk. Selsk. Mat. Fys. Medd. 32, No. 9 (1960).
[25]K. Kumar and M. Baranger, Nucl. Phys. 110, 529 (1968).
[26]R. H. Price, D. G. Burke, and M. W. Johns, Nucl. Phys. A176, 338 (1971).
[27]J. Meyer ter Vehn, F. S. Stephens, and R. M. Diamond, Phys. Rev. Lett. 32, 1383 (1974).
[28]J. Meyer ter Vehn, Nucl. Phys. A249, 141 (1975).
[29]Y. Tanaka and R. K. Sheline, Nucl. Phys. (to be published).